



Seismic properties of the supra-subduction mantle: Constraints from peridotite xenoliths from the Avacha volcano, southern Kamchatka

Vincent Soustelle¹ and Andréa Tommasi¹

Received 30 March 2010; revised 13 May 2010; accepted 7 June 2010; published 10 July 2010.

[1] This work presents seismic properties derived from a detailed microstructural study of supra-subduction mantle xenoliths extracted by the active Avacha volcano in the southern Kamchatka arc. These peridotites underwent low-stress deformation and syn- to late-kinematic reactive percolation of hydrous melts or fluids leading to local orthopyroxene enrichment and dispersion of the olivine CPO in the shallow mantle wedge. All samples show an axial [100] olivine CPO implying fast S-wave polarization parallel to the flow direction in the mantle. Orthopyroxene-enrichment by reactive fluids/melts percolation lowers the Vp/Vs ratio, but cannot explain the Vp/Vs ratios <1.7 mapped in the Japan and Andes forearc mantle. These low Vp/Vs ratios may however be explained by considering the intrinsic anisotropy of the peridotites. **Citation:** Soustelle, V., and A. Tommasi (2010), Seismic properties of the supra-subduction mantle: Constraints from peridotite xenoliths from the Avacha volcano, southern Kamchatka, *Geophys. Res. Lett.*, 37, L13307, doi:10.1029/2010GL043450.

1. Introduction

[2] Seismic data are invaluable tools to probe the thermal structure, flow patterns, and fluid distribution in subduction zones. Seismic anisotropy in the upper mantle depends primarily on the orientation of olivine crystals; splitting measurements using local S-waves may thus record flow directions in the wedge. However, the presence of water and melt may modify the plastic deformation of olivine and hence the relation between seismic anisotropy and mantle flow [Jung and Karato, 2001; Holtzman et al., 2003]. In Kamchatka, fast shear-wave polarization directions vary both along the subduction and with increasing distance to the trench [Levin et al., 2004]. Variable polarization directions and delay times are also observed in other subduction zones, as the Kurils-Japan-Izu Bonin system [e.g., Nakajima and Hasegawa, 2004]. It is fundamental to know if these variations reflect variations in the mantle flow pattern, a change in the dominant olivine intracrystalline deformation mechanism, or result from serpentinization-related processes [Faccenda et al., 2008; Boudier et al., 2010].

[3] The Vp/Vs ratio allows constraining the composition of the mantle wedge. High Vp/Vs ratios may denote the presence of fluids or melts [Takei, 2002]. Low Vp/Vs ratios were attributed to changes in mineralogical composition.

However, highly unusual mantle compositions (involving quartz) were invoked to explain Vp/Vs ratios <1.7 [Wagner et al., 2006, and references therein]. Moreover, the effect of intrinsic anisotropy of mantle rocks on the Vp/Vs ratio is never considered.

[4] We computed the seismic properties of mantle xenoliths from an active subduction zone. They were extracted by the Avacha volcano in southeastern Kamchatka volcanic arc. Their study allows us to determine the active deformation mechanisms in olivine in the presence of hydrous fluids or melts and, hence, to constrain the relation between seismic anisotropy and flow directions in the shallow mantle wedge. It also allows quantification of the effect of the reactive fluids/melts percolation on the seismic properties.

2. Microstructures, Compositions, and Crystal Preferred Orientations

[5] The 23 studied mantle xenoliths come from Holocene andesitic tuffs of the active Avacha volcano located on the southeastern coast of the Kamchatka peninsula. The depths of the Moho and of the top of the subducting slab beneath the Avacha volcano are ca. 35 km and 120 km, respectively [Gorbatov et al., 1997; Levin et al., 2002]. Low P-wave velocities beneath the active volcanic arc are consistent with partial melting in the wedge [Gorbatov et al., 1999]. Splitting measurements on local shear waves in southeastern Kamchatka yield trench-normal and trench-parallel polarization of fast S-waves in the fore-arc and the back-arc, respectively [Levin et al., 2004].

[6] These Avacha peridotite xenoliths were the subject of detailed petrological [Ionov, 2010] and microstructural [Soustelle et al., 2010] studies. They are highly refractory harzburgites (>3% clinopyroxene) formed by high degrees of melting (28–35%) at relatively low pressures (1–2 GPa). They display a coarse-grained porphyroclastic texture with a well-developed lineation marked by spinel trails and large elongated olivine crystals (1–5 mm long). Olivine crystals have curvilinear grain boundaries that locally evolve into polygonal shapes with 120° triple junctions, widely-spaced (100) subgrain boundaries, and low free dislocation densities. These microstructures are characteristic of diffusion-assisted dislocation creep, suggesting deformation under low-stress, high-temperature conditions. Two-pyroxenes equilibrium temperatures around 800–900°C [Ionov, 2010] imply that the low-stress “asthenospheric” deformation was followed by cooling and addition to the overriding plate lithosphere from where the xenoliths were extracted.

[7] One third of the studied xenoliths are slightly enriched in Si and show rather high orthopyroxene modal contents (18–30%). In some samples, orthopyroxene tends to con-

¹Géosciences Montpellier, Université Montpellier II, CNRS, Montpellier, France.

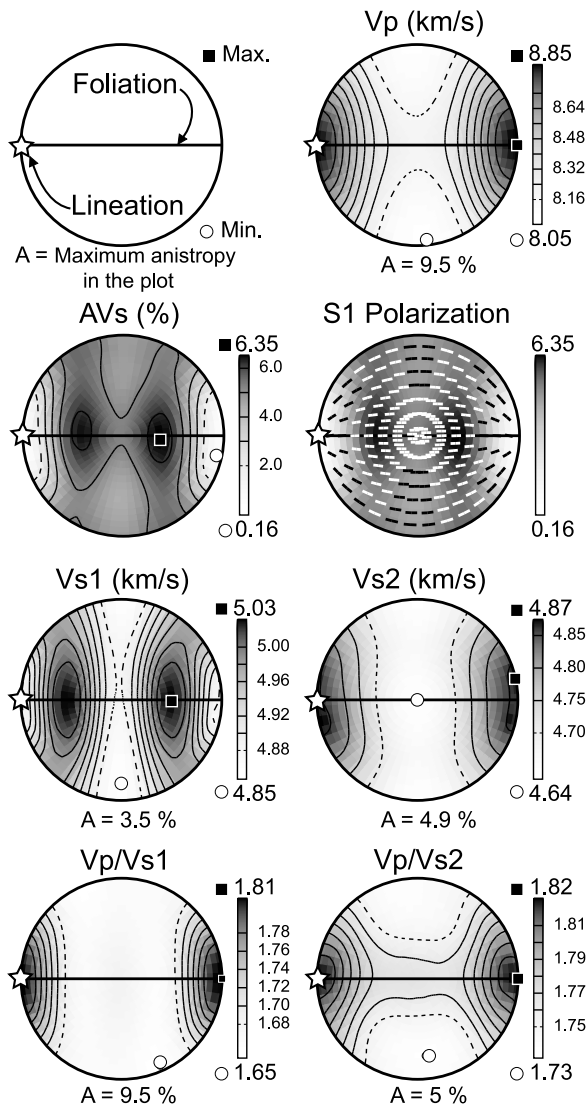


Figure 1. Seismic properties of an average sample obtained by summation of the CPO of 23 peridotite xenoliths. From left to right and top to bottom, schematic representation of the foliation/lineation reference frame used in this study, variation as a function of the propagation direction of the compressive waves velocities (V_p in km/s), of the intensity of the shear wave polarization anisotropy ($AV_s = 200 \cdot (V_{s1} - V_{s2}) / (V_{s1} + V_{s2})$ in %), of the polarization of the fast shear wave S_1 (grey scale represents the intensity of AV_s , as in the previous plot), of the two quasi-shear waves (V_{s1} and V_{s2}) velocities, and of the V_p/V_{s1} and V_p/V_{s2} ratios. Equal area, lower hemisphere stereographic projections.

centrate in lenses parallel to the foliation. Based on the analysis of the microstructures, *Soustelle et al.* [2010] proposed that orthopyroxene enrichment resulted from syn- to late kinematic reactive percolation of a Si-rich melt/fluid leading to orthopyroxene crystallization at the expense of olivine.

[8] Olivine CPO obtained by electron backscattered diffraction (EBSD) [*Soustelle et al.*, 2010] show well-developed axial-[100] patterns characterized by alignment of [100] parallel to the lineation, and girdle distributions of [010] and

[001] normal to it, pointing to dominant [100] slip on multiple $\{0kl\}$ planes, mainly (010) and (001). Activation of [100] slip on multiple planes is consistent with the maximum water contents in olivine (13–28 wt ppm H_2O) estimated from IR spectroscopy measurements [*Soustelle et al.*, 2010] and with deformation at moderate pressures, in the spinel stability field [*Mainprice et al.*, 2005]. The highly variable orthopyroxene CPO, which may either be correlated or not with the olivine CPO, and the decrease of the intensity of the olivine CPO in opx-rich samples corroborate the syn- to late kinematic character of the reactive fluid transport [*Soustelle et al.*, 2010].

3. Seismic Properties

[9] The three-dimensional distributions of seismic velocities have been computed by averaging the individual grain elastic constants tensor as a function of the crystallographic orientation given by the EBSD measurements and modal composition [*Mainprice and Humbert*, 1994]. We used Voigt-Reuss-Hill averaging and single-crystal elastic constants tensors of olivine and orthopyroxene at ambient conditions [*Duffy and Vaughan*, 1988; *Abramson et al.*, 1997].

[10] As seismic waves sample the anisotropy at length scales ranging from a few to a thousand of kilometers, we calculate seismic properties for an average harzburgite sample obtained by summation of the CPO of the 23 individual samples. For summation, all individual CPO were rotated as to have the lineation and the pole of the foliation in the E-W and N-S directions, respectively. 3D-seismic properties of the average sample (Figure 1) are very similar to those of individual xenoliths (not shown here). P- and S_2 -waves propagation is fastest parallel to the lineation and slowest in the plane normal to the lineation. S_1 -wave velocity is minimum for propagation directions both parallel and normal to the lineation and maximum at $\sim 45^\circ$ to the lineation in the foliation plane. S-wave splitting is minimum for waves propagating at low angle to the lineation and highest for waves propagating at high angles ($\geq 30^\circ$) to the lineation in the foliation plane. S-waves propagating normal to the foliation also sample a high birefringence direction. For all propagation directions, the fast S-wave is polarized parallel to the lineation. This anisotropy pattern is typical of peridotites which olivine CPO has an orthorhombic or axial [100] symmetry [*Tommasi et al.*, 2004; *Vauchez et al.*, 2005]. It is also in good agreement with the seismic properties calculated for another Avacha volcano xenolith collection by *Michibayashi et al.* [2009]. Moreover, V_p/V_{s1} and V_p/V_{s2} ratios are minimum for propagation directions at high angle ($>30^\circ$) to the lineation and the foliation, respectively. Both ratios are maximum parallel to the lineation.

[11] In Avacha xenoliths, syn- to late kinematic reactive percolation resulted in crystallization of orthopyroxene at the expense of olivine. To quantify the effect of this process, we analyze the evolution of the P-wave azimuthal anisotropy and S-wave polarization anisotropy (splitting) as a function of the orthopyroxene modal content in the studied samples (Figure 2). Two groups may be discriminated: (1) Harzburgites with “normal” opx contents ($<21\%$) display P-wave anisotropy and S-waves splitting maxima ranging from 14 to 10% and 9.5 to 6%, respectively. (2) Harzburgites enriched in opx ($>21\%$) show lower and less variable

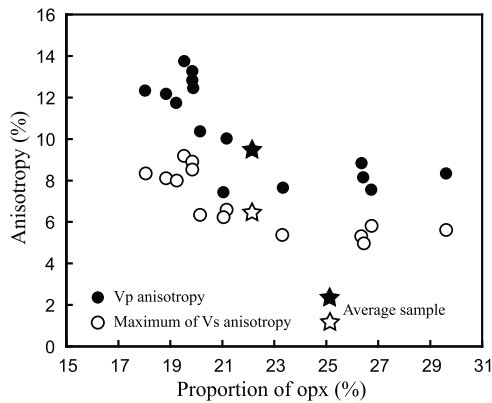


Figure 2. P- and maximum S-wave anisotropy as a function of the orthopyroxene content in 15 Avacha peridotite xenoliths for which the modal composition has been accurately determined.

P-wave anisotropy and S-waves splitting maxima of 6.5–9% and 5.5–6.5%, respectively.

4. Discussion

4.1. Seismic Anisotropy and Flow Directions in the Mantle Wedge Beneath Kamchatka

[12] The determination of the dominant deformation mechanisms in olivine is fundamental to deduce flow patterns in the mantle from S-waves anisotropy data. Through the analysis of the CPO and microstructures of the Avacha xenoliths, *Soustelle et al.* [2010] showed that even if the samples were percolated by hydrous melts/fluids, olivine had moderate water contents and deformed essentially by [100] slip assisted by diffusional processes. The resulting axial [100] olivine CPO patterns in the Kamchatka peridotite xenoliths imply that for all propagation directions the fast S-wave is polarized parallel to the lineation or the flow direction (Figure 1). The presence of hydrous melts or fluids has therefore no impact on the fast S-waves polarization directions in the shallow mantle wedge and S-waves splitting data can be used to map the horizontal component of the mantle flow. The present study thus corroborates the interpretation of *Levin et al.* [2004] that ascribed the trench-normal fast polarizations beneath the southern part of the Kamchatka arc to a local corner flow. The corner flow probably does not extend inland beyond the arc, since stations in the back-arc domain show trench-parallel fast polarizations.

4.2. Effect of Reactive Melt/Fluid Percolation on Seismic Anisotropy

[13] Syn-deformation reactive melt/fluid percolation lead to orthopyroxene enrichment, dispersion of the olivine CPO, and decrease in seismic anisotropy in 1/3 of the Avacha xenoliths (Figure 2). The average S-wave anisotropy maximum in “normal” harzburgites is 8%, whereas the average over the entire suite, including the opx-enriched harzburgites, is 6.35%. Reactive transport of hydrous fluids or melts during mantle deformation may thus decrease anisotropy by up to 20%. Splitting measurements in southern Kamchatka using local shear waves yield delay times between 0 and 1.5 s with a peak at 0.5 s [*Levin et al.*, 2004]. If we assume

that the “normal” harzburgites represent the typical upper mantle wedge, delay times of 0.5, 1, and 1.5 s for a mean $V_s = 4.5 \text{ km.s}^{-1}$ are produced by 28, 56, and 84 km long paths along the foliation at high angle to the lineation (other propagation directions relative to the structural reference frame sample lower intrinsic anisotropies and require thicker anisotropic layers to produce the same delay times, cf. Figure 1). Minimum anisotropic paths needed to produce the same delay times are however 35, 71, and 106 km long if the average sample birefringence is considered. Thus if large volumes of the wedge mantle were modified by reactive fluid percolation leading to an anisotropy decrease similar to the one observed in the Kamchatka orthopyroxene-rich harzburgites, 26% longer anisotropic paths or an additional contribution from the slab or the crust of the upper plate are required to produce the observed delay times.

4.3. Significance of Low Vp/Vs Ratios in the Mantle Wedge

[14] Vp/Vs ratios mapped by seismic tomography models in subduction zones are highly variable, ranging from 1.6 to 1.95 [*Zhang et al.*, 2004; *Wagner et al.*, 2005]. The average Vp/Vs in the shallow upper mantle is 1.73–1.75. High Vp/Vs (>1.8) are characteristic of processes leading to a stronger decrease in S-waves velocities relatively to P-waves; they are traditionally interpreted as recording the presence of melts, fluids [*Takei*, 2002], or serpentine [*Christensen*, 1996] in the mantle wedge.

[15] The processes producing low Vp/Vs ratios (<1.7) in subduction zones are, in contrast, poorly constrained. Such low Vp/Vs ratios are nevertheless observed in tens of km wide domains in the fore-arc mantle from Japan, Andes and Alaska subduction zones [*Zhang et al.*, 2004; *Rossi et al.*, 2006; *Wagner et al.*, 2006]. Different models were proposed to explain these observations, like the presence of quartz [*Rossi et al.*, 2006; *Wagner et al.*, 2006] or orthopyroxene enrichment [*Zhang et al.*, 2004; *Wagner et al.*, 2006].

[16] Based on the analysis of the microstructures and modal compositions of the Avacha xenoliths, *Soustelle et al.* [2010] proposed that reactive percolation leads to local enrichment in orthopyroxene in the mantle wedge. To quantify if the observed orthopyroxene enrichment may account for the observed low Vp/Vs ratios, we calculated the Vp/Vs ratios for the Avacha peridotites. Because body-wave tomographic models, from which Vp/Vs ratios are extracted, usually neglect seismic anisotropy, we first calculated the seismic properties of isotropic aggregates with the same modal composition as the studied samples. S-wave velocities are almost insensitive to the orthopyroxene enrichment, whereas P-waves velocities strongly decrease with increasing orthopyroxene contents, leading to a decrease of the Vp/Vs ratio (Figure 3a). The variation in Vp/Vs ratio produced by an orthopyroxene enrichment similar to the one observed in the Avacha peridotite xenoliths is similar to the one induced by an increase in pressure by 1 GPa or a decrease in temperature by $\sim 300^\circ\text{C}$ (Figure 3b). The minimum Vp/Vs ratio obtained for the most opx-enriched composition sampled by the Avacha peridotites (30% opx) is 1.72. This ratio is higher than those observed in tens of km wide domains of the fore-arc mantle from the Japan and Andes subduction zones (1.65–1.7 [*Zhang et al.*, 2004; *Wagner et al.*, 2006]). To explain these ratios, large areas of

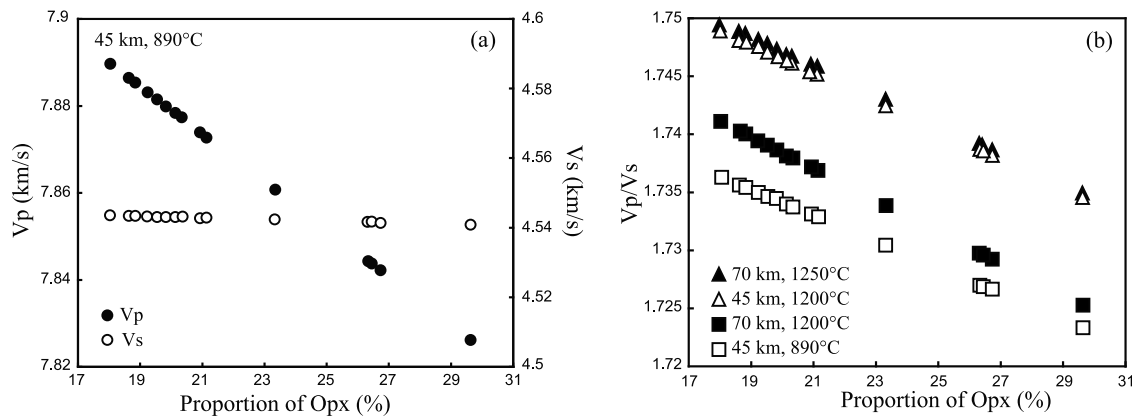


Figure 3. (a) P- and S-waves velocities, and (b) Vp/Vs ratios for different depths and temperatures in an isotropic harzburgite (random olivine CPO) with variable orthopyroxene modal contents.

the mantle wedge should have an orthopyroxenite composition (>90% opx), which is unrealistic. Indeed, orthopyroxenites are only observed as thin dykes, a few cm to tens of cm wide, in both xenoliths and peridotite massifs [e.g., Tommasi *et al.*, 2006; Soustelle *et al.*, 2010].

[17] Low Vp/Vs ratios in the upper mantle may however be understood by considering the anisotropy of seismic properties of deformed peridotites. The average Avacha peridotite sample displays indeed a strong variation of the Vp/Vs₁ and Vp/Vs₂ ratios as a function of the propagation direction: the Vp/Vs₁ ratio is <1.7 for all propagation directions at angles >30° to the lineation (Figure 1).

[18] How are “isotropic” Vp/Vs ratios measured in an anisotropic mantle? Vp/Vs ratios are determined by picking the first S-wave arrival on the transverse component [e.g., Wagner *et al.*, 2005], which usually corresponds to the S1 wave. Only in the special case where the initial polarization, which depends essentially on the focal mechanism, is along the S2 direction there will be no energy in the S1 direction. Deformation in mantle wedge is usually defined as a combination of corner and trench-parallel flow, resulting from entrainment by the downgoing slab and geometrical complexities of the plates’ boundary geometry or oblique convergence, respectively. The latter induces horizontal lineations in the fore-arc mantle, whereas corner-flow produces lineations that range between horizontal and shallow to steeply-deeping depending on the proximity to the slab and on the slab dip. This implies that most seismic rays produced by local earthquakes cross the mantle wedge at high angle to the lineation [Kneller and van Keken, 2008]. Thus, the measured “isotropic” Vp/Vs ratio is most often the Vp/Vs₁ ratio, which is <1.7 in all domains of the mantle wedge with a horizontal to shallowly-deeping lineation, unless fluids, melts or serpentinization are present.

5. Conclusion

[19] Peridotite xenoliths sampling the sub-arc mantle in the Kamchatka subduction zone show high-temperature, low-stress deformation microstructures and axial [100] olivine CPO, pointing to deformation by dislocation creep with dominant activation of [100] glide, consistent with the measured moderate water contents in olivine. Thus if anisotropy in the mantle wedge results essentially from olivine deformation, the fast S-waves polarization will be

parallel to the flow direction. Synkinematic porous flow of melts or fluids may favor diffusion leading to weaker olivine CPO and locally lower the anisotropy.

[20] More important, reactive percolation of Si-rich fluids or hydrous melts in the wedge results in crystallization of orthopyroxene at the expenses of olivine. Opx-enrichment induces a limited decrease in the Vp/Vs ratio, but cannot explain the Vp/Vs ratios <1.7 observed in many subduction wedges. The latter may nevertheless be accounted for by considering the intrinsic anisotropy of deformed peridotites.

[21] **Acknowledgments.** V.S. and A.T. thank D. Mainprice for providing softwares for calculating seismic properties of anisotropic rocks, C. Tiberi for discussions on measurements of Vp/Vs ratios, Martha Savage and an anonymous referee for their constructive reviews. This study was partially funded by the program SEDIT of the Institut National des Sciences de l’Univers (INSU-CNRS), France, in the frame of the project “Deformation in the supra-subduction mantle” coordinated by A.T. V.S. benefited from a PhD scholarship from the Ministère de la Recherche et de l’Enseignement Supérieur, France.

References

- Abramson, E. H., J. M. Brown, L. J. Slutsky, and J. Zaugg (1997), The elastic constants of San Carlos olivine to 17 GPa, *J. Geophys. Res.*, *102*, 12,253–12,263, doi:10.1029/97JB00682.
- Boudier, F., A. Baronnat, and D. Mainprice (2010), Serpentine mineral replacements of natural olivine and their seismic implications: Oceanic lizardite versus subduction-related antigorite, *J. Petrol.*, *51*, 495–512, doi:10.1093/petrology/egp049.
- Christensen, S. I. (1996), Poisson’s ratio and crustal seismology, *J. Geophys. Res.*, *101*, 3139–3156, doi:10.1029/95JB03446.
- Duffy, T. S., and M. T. Vaughan (1988), Elasticity of enstatite and its relationships to crystal structure, *J. Geophys. Res.*, *93*, 383–391, doi:10.1029/JB093iB01p00383.
- Faccenda, M., L. Burlini, and D. Mainprice (2008), Fault-induced seismic anisotropy by hydration in subduction oceanic plates, *Nature*, *455*, 1097–1100, doi:10.1038/nature07376.
- Gorbatov, A., V. Kostoglodov, G. Suárez, and E. Gordeev (1997), Seismicity and structure of the Kamchatka subduction zone, *J. Geophys. Res.*, *102*, 17,883–17,898, doi:10.1029/96JB03491.
- Gorbatov, A., J. Dominguez, G. Suarez, V. Kostoglodov, D. Zhao, and E. Gordeev (1999), Tomographic imaging of the P-wave velocity structure beneath the Kamchatka peninsula, *Geophys. J. Int.*, *137*, 269–279, doi:10.1046/j.1365-246X.1999.00801.x.
- Holtzman, B. K., D. L. Kohlstedt, M. E. Zimmerman, F. Heidelbach, T. Hiraga, and J. Hustoft (2003), Melt segregation and strain partitioning: Implications for seismic anisotropy and mantle flow, *Science*, *301*, 1227–1230, doi:10.1126/science.1087132.
- Ionov, D. A. (2010), Petrology of mantle wedge lithosphere: New data on supra-subduction zone peridotite xenoliths from the andesitic Avacha volcano, Kamchatka, *J. Petrol.*, *51*, 327–361, doi:10.1093/petrology/egp090.

- Jung, H., and S. Karato (2001), Water-induced fabric transitions in olivine, *Science*, *293*, 1460–1463, doi:10.1126/science.1062235.
- Kneller, E. A., and P. E. van Keken (2008), The effects of three-dimensional slab geometry on deformation in the mantle wedge: Implications for shear wave anisotropy, *Geochem. Geophys. Geosyst.*, *9*, Q01003, doi:10.1029/2007GC001677.
- Levin, V., J. Park, M. Brandon, J. Lees, V. Peyton, E. Gordeev, and A. Ozerov (2002), Crust and upper mantle of Kamchatka from teleseismic receiver functions, *Tectonophysics*, *358*, 233–265, doi:10.1016/S0040-1951(02)00426-2.
- Levin, V., D. Droznin, J. Park, and E. Gordeev (2004), Detailed mapping of seismic anisotropy with local shear waves in southeastern Kamchatka, *Geophys. J. Int.*, *158*, 1009–1023, doi:10.1111/j.1365-246X.2004.02352.x.
- Mainprice, D., and M. Humbert (1994), Methods of calculating petrophysical properties from lattice preferred orientation data, *Surv. Geophys.*, *15*, 575–592, doi:10.1007/BF00690175.
- Mainprice, D., A. Tommasi, H. Couvy, P. Cordier, and D. J. Frost (2005), Pressure sensitivity of olivine slip systems and seismic anisotropy of Earth's upper mantle, *Nature*, *433*, 731–733, doi:10.1038/nature03266.
- Michibayashi, K., T. Oohara, T. Satsukawa, S. Ishimaru, S. Arai, and V. Okrugin (2009), Rock seismic anisotropy of the low-velocity zone beneath the volcanic front in the mantle wedge, *Geophys. Res. Lett.*, *36*, L12305, doi:10.1029/2009GL038527.
- Nakajima, J., and A. Hasegawa (2004), Shear-wave polarization anisotropy and subduction-induced flow in the mantle wedge of northeastern Japan, *Earth Planet. Sci. Lett.*, *225*, 365–377, doi:10.1016/j.epsl.2004.06.011.
- Rossi, G., G. A. Abers, S. Rondenay, and D. H. Christensen (2006), Unusual mantle Poisson's ratio, subduction, and crustal structure in central Alaska, *J. Geophys. Res.*, *111*, B09311, doi:10.1029/2005JB003956.
- Soustelle, V., A. Tommasi, S. Demouchy, and D. A. Ionov (2010), Deformation and fluid-rock interaction in the supra-subduction mantle: Microstructures and water contents in peridotite xenoliths from the Avacha Volcano, Kamchatka, *J. Petrol.*, *51*, 363–394, doi:10.1093/ptrology/egp085.
- Takei, Y. (2002), Effect of pore geometry on V_p/V_s : From equilibrium geometry to crack, *J. Geophys. Res.*, *107*(B2), 2043, doi:10.1029/2001JB000522.
- Tommasi, A., M. Godard, G. Coromina, J. M. Dautria, and H. Barszczus (2004), Seismic anisotropy and compositionally induced velocity anomalies in the lithosphere above mantle plumes: A petrological and microstructural study of mantle xenoliths from French Polynesia, *Earth Planet. Sci. Lett.*, *227*, 539–556, doi:10.1016/j.epsl.2004.09.019.
- Tommasi, A., A. Vauchez, M. Godard, and F. Belley (2006), Deformation and melt transport in a highly depleted peridotite massif from the Canadian Cordillera: Implications to seismic anisotropy above subduction zones, *Earth Planet. Sci. Lett.*, *252*, 245–259, doi:10.1016/j.epsl.2006.09.042.
- Vauchez, A., F. Dineur, and R. Rudnick (2005), Microstructure, texture and seismic anisotropy of the lithospheric mantle above a mantle plume: Insights from the Labait volcano xenoliths (Tanzania), *Earth Planet. Sci. Lett.*, *232*, 295–314, doi:10.1016/j.epsl.2005.01.024.
- Wagner, L. S., S. Beck, and G. Zandt (2005), Upper mantle structure in the south central Chilean subduction zone (30° to 36°S), *J. Geophys. Res.*, *110*, B01308, doi:10.1029/2004JB003238.
- Wagner, L. S., S. Beck, G. Zandt, and M. N. Ducea (2006), Depleted lithosphere, cold, trapped asthenosphere, and frozen melt puddles above the flat slab in central Chile and Argentina, *Earth Planet. Sci. Lett.*, *245*, 289–301, doi:10.1016/j.epsl.2006.02.014.
- Zhang, H., C. H. Thurber, D. Shelly, S. Ide, G. C. Beroza, and A. Hasegawa (2004), High-resolution subducting-slab structure beneath northern Honshu, Japan, revealed by double-difference tomography, *Geology*, *32*, 361–364, doi:10.1130/G20261.2.

V. Soustelle and A. Tommasi, Géosciences Montpellier, Université Montpellier II, CNRS, CC 60, Place E. Bataillon, F-34095 Montpellier CEDEX 5, France. (vsoustel@gm.univ-montp2.fr)